Fully integrated whole blood testing by real-time absorption measurement on a centrifugal platform

J. Steigert,*[a] M. Grumann,[a] T. Brenner,[a] L. Riegger,[a] J. Harter,[a] R. Zengerle[ab] and J. Ducrée[ab]

Received 17th May 2006, Accepted 17th May 2006
First published as an Advance Article on the web 5th June 2006
DOI: 10.1039/b607051p

We present a novel microfluidic concept to enable a fast colorimetric alcohol assay from a single droplet of whole blood. The reduced turn-around time of 150 seconds is, on the one hand, achieved by a full process integration including metering, mixing with reagents, and sedimentation of cellular constituents. On the other hand, our novel total internal reflection (TIR) scheme allows to monitor the increase of the absorbance values in real-time. Thus, the saturation values can be predicted accurately based on an extrapolation of real-time measurements acquired during a 100 second initial period of rotation. Additionally, we present a metering structure to define nanolitre sample volumes at a coefficient of variation (CV) below 5%.

Introduction

The transfer of procedures in clinical diagnostics to compact point-of-care devices is subject of various academic and commercial efforts. Microfluidics are considered as a key technology within the promising sector of medical diagnostics especially for point-of-care applications.[1–5] To meet the stringent requirements of clinical diagnostics, miniaturized 'lab-on-a-chip' technologies featuring a full process integration, reduced consumption of sample and reagents, as well as short turn-around times and ease of handling are the most prominent candidates.[6–12] Several of these microfluidic technologies are highly competitive with or even superior to conventional laboratory-scale technologies.

Among these 'lab-on-a-chip' systems, we here consider centrifugal 'lab-on-a-disk' technologies which exploit the interplay of centrifugal and capillary forces to fully integrate analytical protocols comprising the entire process chain, *e.g.* sample preparation, mixing, reaction, separation and detection.[13–23] Numerous 'lab-on-a-disk' products have already been launched to the market.[24–30]

In this work, we focus on the implementation of a disk-based, colorimetric alcohol assay on human whole blood with monolithically integrated optical beam-guidance to enhance the sensitivity by total-internal-reflection (TIR). The alcohol concentration is one of the most relevant markers in toxicology, especially in emergency diagnostics. Furthermore, alcohol detection helps to improve existing protective and safety measures in law enforcement agencies, community and work environments. With our setup we avoid the error-prone determination known from common breath analyzers. A reduced time-to-result is achieved by real-time measurement of the reaction kinetics and extrapolation to accurately predict the saturation values. To enhance the quality of our assay, we additionally present a novel metering structure based on capillary burst valves to define the sample volume very precisely, by tailoring a tiny tear-off meniscus.

[a]*University of Freiburg - IMTEK, Department of Microsystems Engineering, Laboratory for MEMS Applications, Georges-Koehler-Allee 106, D-79110, Freiburg, Germany. E-mail: steigert@imtek.de; Fax: +49-761-203-7539; Tel: +49-761-203-7476*
[b]*HSG-IMIT - Institute for Micromachining and Information Technology, Wilhelm-Schickard-Strasse 10, D-79110, Villingen-Schwenningen, Germany*

Optical setup

Colorimetric assays are based on the measurement of the intensity I of a probe beam of an incident intensity I_0 after passing the detection cell containing the analyte solution. According to the law of Beer–Lambert, the absorbance (or optical density) linearly depends on the molar extinction coefficient $\varepsilon(\lambda)$ of the solution (which is governed by the products of the colorimetric reaction), the initial concentration c, and the optical path length l_{abs} through the detection cell.

$$A = \log\left(\frac{I_0}{I}\right) = \ln(10)\ \varepsilon(\lambda)\ c\ l_{abs} \quad (1)$$

In miniaturized formats, the sensitivity thus suffers form the significantly reduced optical path length l_{abs} compared to macroscopic setups. Several approaches to extend the optical path length l_{abs} by an optical on-chip guidance of the interrogating beam on flat microfluidic chips accommodating low-aspect-ratios have been pursued[31] *e.g.* based on embedded optical waveguides[32,33] integrated microlenses,[34] optical fibers[35,36] or total-internal-reflection in silicon micro mechanics.[37–39] However, these approaches require rather complex chip designs and an elaborate, high-accuracy alignment of the optical components.

In our rugged optical setup[40] the optical beam of a laser (λ_{peak} = 530 nm)[41] is directed at perpendicular incidence on the flat upper side of the polymer (COC) disk. At the symmetric side faces of the triangular V-grooves which are monolithically embedded into the reverse side of the disk, the impinging laser beam is deflected *via* total internal reflection (TIR) by 90° into the plane of the detection cell (Fig. 1). To ensure TIR, the angle of incidence α has to exceed the critical angle α_c which is governed by the refractive indices of the polymer substrate $n_{COC} \approx 1.5$ and the surrounding air n_{air}. Thus, the angle of

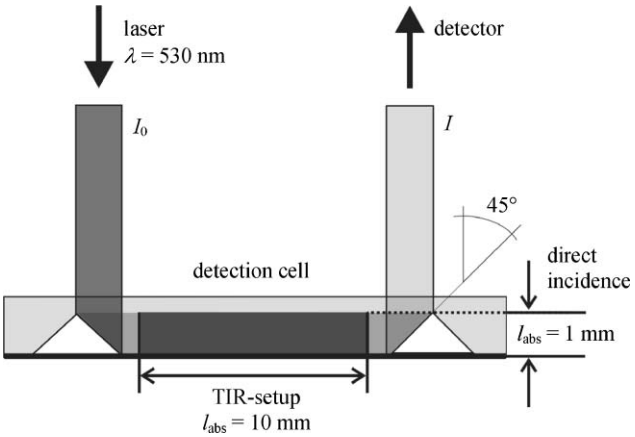

Fig. 1 Monolithically integrated V-grooves next to the measurement chamber perpendicularly deflect the probe beam of initial intensity I_0 by total internal reflection into the disk plane. This method allows to significantly extend the optical path length l_{abs}. After passing the detection chamber, the attenuated intensity of the probe beam I is measured by a detector positioned above the disk. To ensure TIR, the incident angle α must be larger than the critical angle $\alpha_c > 41°$.

incidence $\alpha = 45°$ is larger than the calculated critical angle $\alpha_c \approx 41°$. After passing the detection chamber, the attenuated beam is again reflected by 90° at another V-groove towards a spectrophotometer.[42] Thus, absorption takes place along the full length (l_{abs} = 10 mm) of the typically low-aspect-ratio detection cell, instead of the much smaller thickness (l_{abs} = 1 mm) for direct incidence. Compared to direct incidence on flat microfluidic chips, the optical path length and therefore the absorption (eqn (1)) is increased by one order of magnitude.

Alcohol assay

The alcohol concentration c in untreated human whole blood is detected colorimetrically in a two-step enzymatic reaction.[43]

First, the disk is loaded with the reagents namely alcohol oxidase (AOX), horseradish peroxidase (HRP), aminophenazone, and hydroybenzonic acid. In the presence of O_2, AOX catalyzes the oxidation of ethanol while producing stoichiometric amounts of hydrogen peroxide (H_2O_2).

$$\text{Ethanol} + O_2 \xrightarrow{\text{AOX}} \text{acetaldehyde} + H_2O_2 \quad (2)$$

This is followed by a HRP-catalyzed oxidation reaction which correlates linearly with the concentration of H_2O_2.

$$H_2O_2 + \text{4-aminophenazone} + \text{4-hydroxybenzoic acid} \xrightarrow{\text{HRP}} \text{quinoneimine dye} \quad (3)$$

The emergence of the oxidized product is indicated by the evolution of a violet color which is quantified by the decrease of the detected probe beam intensity I (eqn (1)) of a laser emitting at λ_{peak} = 530 nm matching the highest difference in signal amplitude for different c.

Metering

The basic design of the metering structure is based on two capillary burst valves.[44,45] The first is located at the outlet of the metering chamber to define a liquid volume confined at the upstream end by the intersecting overflow channel (Fig. 2A). The second hydrophobic barrier is placed at the outlet of the overflow channel. Due to the enhanced height of the upstream liquid column and the increased channel cross section, this valve yields at a lower burst frequency as the other capillary barrier.

With the disk at rest, the entire fluidic network is primed by capillary action with an undefined (excess) sample volume up to the capillary valves. Spinning at ν = 10 Hz, the hydrophobic barrier in the overflow channel brakes and the residual liquid is cut off and purged into the waste chamber (Fig. 2B). Surpassing the burst frequency ν = 35 Hz > ν_c of the barrier at

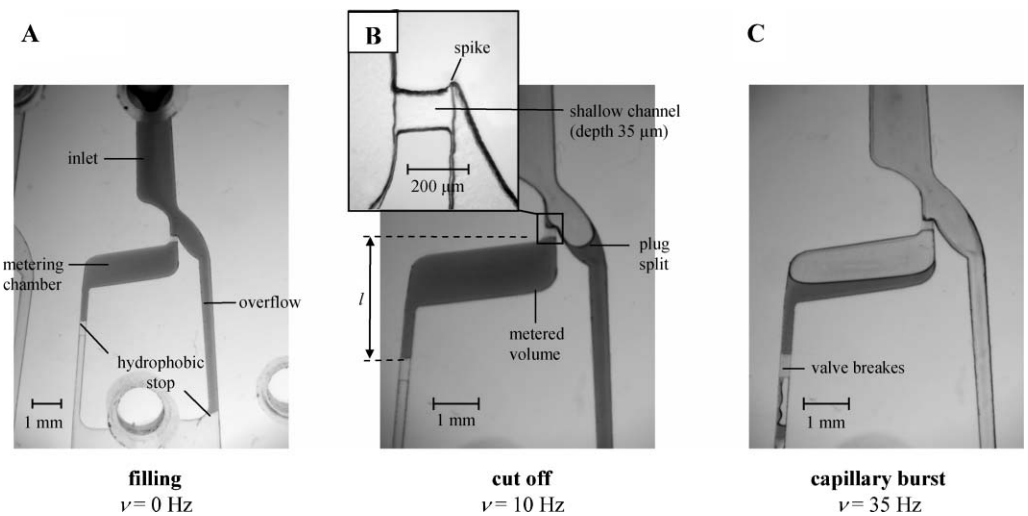

Fig. 2 Sequence showing the course of metering and valving, only controlled by the spinning frequency ν. (A) At ν = 0 Hz, the structure is primed by capillary force until the menisci stop at the hydrophobic patches. (B) At ν = 10 Hz, the hydrophobic stop at the outer end of the overflow breaks and the liquid in the inlet drains into the overflow. When the receding meniscus passes the junction between overflow and metering chamber, the plug sharply splits at the shallow channel segment. This way, the plug length l and the metered volume is clearly defined. (C) At 35 Hz, the centrifugal pressure induced on the liquid column in the metering chamber exceeds the capillary pressures and the valve brakes.

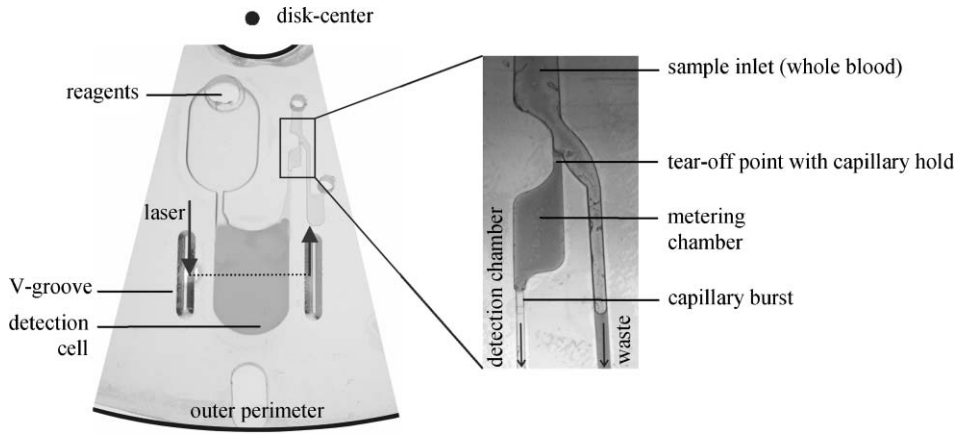

Fig. 3 Concept of a disk-based alcohol assay on a sample of human whole blood. The microfluidic polymer disk (COC) in the format of a conventional CD hosts a metering structure to define a sample volume (V_s = 0.5 μL) and an inlet for the reagents (V_r = 99.5 μL) which are connected to the measurement chamber. The sample volume is metered at high precision (CV < 5%) by tailoring a tiny tear-off meniscus.

the end of the metering chamber, the liquid is purged into the detection chamber (Fig. 2C).

The precision and reproducibility of the metered volume is decisively impacted by break-off process cut at the intersection of the overflow with the inlet of the metering chamber. To understand this important effect, we briefly picture the course of the break-off process. After priming, the liquid volumes in the metering chamber and the overflow channels communicate by a continuous liquid column, or at least some capillary flow along the edges the channels ('wicking').

To counteract this parasitic effect, we minimize the dead volume in the intersection and cut-off the liquid connection between the two structures. To this end, the intersection is represented by knife-like edge to interrupt the liquid flow and a shallow, hydrophilic channel segment at the entrance of the metering chamber to subsequently pin the emerging meniscus.

Based on these features, we designed metering structures from the μL-range down to the nL-range exhibiting an extremely high reproducibility, *e.g.* a 300 nL volume is metered with a quality of CV < 5%. The volume quantification is implemented by processing the digital images taken by a stroboscopic camera setup.[46] First, the parts filled with liquid were selected. Then the pixel count was computed according to the size of the measured geometry. Finally, the count was mathematically translated into a volume.[47] The well defined metering of the sample volume is crucial for the quantification of the colorimetric reaction and thus for the reproducibility of the assay results.

So far, systems for the precise metering of small volumes in the nL-range have been presented and also integrated into blood analysis devices,[48–50] *e.g.* home tests to determine the glucose or cholesterol levels. These structures are based on a filtration of the red blood cells out off the plasma and a metering by a defined channel length. In comparison, our principle allows to meter a wide range of liquid volumes. Furthermore, as metering constitutes a fundamental step in quantitative assays, the presented metering structure could easily be combined with other unit operations (*e.g.* sedimentation, mixing, incubation) to integrate more complex assay protocols on a single chip.

Assay protocol

After loading the reagents into the inlet reservoirs (Fig. 3), a droplet of untreated human blood is extracted from the fingertip and directly loaded onto the disk. Then, all steps of the alcohol assay are implemented by a fully automated frequency protocol $v(t)$ (Fig. 4). This way, error prone handling steps are eliminated.

First, a small 500 nL volume blood sample is metered very precisely, before the disk is spun at v = 35 Hz > v_c to break the capillary burst-valves and transport the liquids into the detection chamber.

To enforce rapid mixing the sense of rotation is frequently reversed. This so-called 'shake-mode' has proven to accelerate

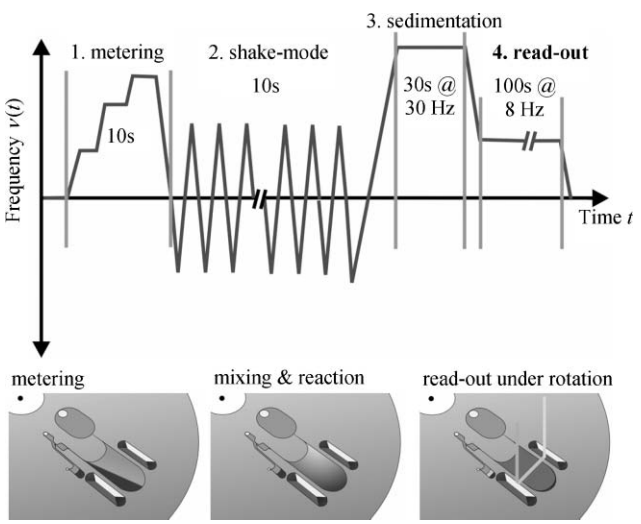

Fig. 4 Frequency protocol $v(t)$ performing an on-disk alcohol-assay within t = 150 s. The ethanol concentration in human whole blood is determined colorimetrically. After the sample and the reagents are loaded into the inlet reservoirs, the disk is spun and the sample is metered before the liquids are transported into the measurement chamber (1). Frequent changes of the sense of rotation ('shake-mode') accelerate mixing (2) for the enzymatic reaction. The RBCs then sediment out of the optical beam path (3) and the assay is read out in real-time under spinning at a constant frequency of rotation (4).

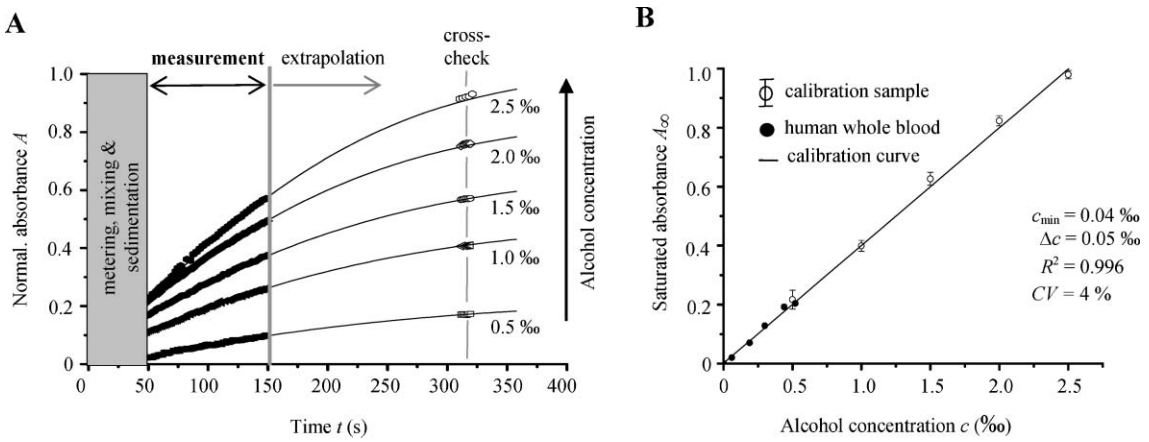

Fig. 5 Real-time read-out of an alcohol assay to shorten the time-to-result (τ = 150 s). (A) After mixing and sedimentation is completed, the increase of the absorbance A is recorded for 100 s and the saturation value A_∞ is extrapolated by a regression fit based on measured values between 50 s and 150 s. (B) The extrapolated values are in good agreement with the saturation values derived for standard ethanol solutions.

mixing in this particular layout from 6.5 minutes for mere diffusion to 5 s.[51] The disk is then spun at v = 30 Hz for 90 s to clear the cellular constituents of the blood, mainly red blood cells (RBCs), from the optical beam path. The RBCs would otherwise interfere with the optical detection. After all necessary assay steps are conducted, the absorbance values are monitored in real-time for 100 s at 8 Hz.

Results

After sedimentation, the absorbance A is monitored in real-time during constant spinning for about 100 s. The acquired data points are then extrapolated by a regression fit to the saturated absorbance value A_∞ (Fig. 5A). The absorption characteristics well complies with the law of Beer–Lambert (Fig. 5B). The assay was benchmarked with calibrated samples.[52] Our measurements display a CV of 4.0%, a low limit of detection (c_{min} = 0.04‰), an excellent resolution (Δc = 0.05‰), and a high linearity between the alcohol concentration and the optical signal (R^2 = 0.996) (Fig. 5B). The measured alcohol concentrations c well agree with the reference measurements.[53] Furthermore, the real time monitoring under rotation allows to accurately predict the saturation value of the enzymatic reaction, which is reached after about 6–8 minutes in standard kits, within about 100 seconds, only. This performance is comparable to common breath analyzers while avoiding the error-prone correlation between the alcohol concentration in breath and whole blood.

Conclusion

We introduced a highly process integrated, disk-based assay to rapidly and accurately determine the concentration of alcohol in human whole blood. The assay is run on a cost-efficient modular platform comprising a passive polymer disk with intaglioed optical and fluidic structures as well as a standard laser diode and detector. Our newly integrated metering structure defines a small sample volume at high accuracy (CV $<$ 5%). This allows a fully automated assay protocol which eliminates error prone handling steps. The results are comparable to common point-of-care tests. Its high degree of automation, its short time-to-result and its excellent precision recommend our centrifugal platform for point-of-use testing and routine screening in clinical labs.

Thus, our setup is readily amenable for porting common applications to small bench scale platforms. In the future, the alcohol assay will be combined with other colorimetric assays at different probe wavelengths. The generic rotational symmetry of the disk suggest to place several channels on the same disk which can be used to process a set of protocols sequentially or even simultaneously.

Acknowledgements

The authors thank the federal state of Baden-Württemberg (contract 24-720.431-1-7/2) for partial financial support of this project. As well as the HSG-IMIT,[54] Jobst-Technologies,[55] and Ulrich Stumm for their good cooperation.

References

1 J. Ducrée and R. Zengerle, in *Flow Map–Microfluidics Roadmap for the Life Sciences*, Books on Demand GmbH, Nordstedt, 2004, ISBN: 3833407441.
2 T. H. Schulte, R. L. Bardell and P. H. Weigl, Microfluidic technologies in clinical diagnostics, *Clin. Chim. Acta*, 2002, **321**, 1–10.
3 S. Sia, V. Linder, B. Parviz, A. Siegel and G. Whitesides, An integrated approach to a portable and low-cost immunoassay for resource-poor settings, *Angew. Chem., Int. Ed.*, 2004, **43**, 498–502.
4 T. Thorsen, S. Markl and S. Quake, Microfluidic large-scale integration, *Anal. Chem.*, 2002, **298**, 580–584.
5 D. Harrison, C. Wang, P. Thibeault, F. Ouchen and S. Cheng, *Proceedings of the 4th International μTAS Conference*, Enschede, 2000, Kluwer Academic Publishers, Dodrecht, The Netherlands, 2000, pp. 195–204.
6 R. E. Oosterbroek and A. van den Berg, in *Lab-on-a-Chip: Miniaturized Systems for (Bio)chemical Analysis and Synthesis*, Elsevier Science, Amsterdam, 2003.
7 T. Vilkner, D. Janasek and A. Manz, Micro total analysis systems; recent developments, *Anal. Chem.*, 2004, **76**, 3373–3386.
8 D. Reyes, D. Iossifidis, P. Auroux and A. Manz, Micro total analysis system 1, *Anal. Chem.*, 2002, **74**, 12, 2623–2636.
9 P. Auroux, D. Reyes, D. Iossifidis and A. Manz, Micro total analysis systems 2, *Anal. Chem.*, 2002, **74**, 2637–2652.

10 A. J. Tudos, G. A. J. Besselink and R. B. M. Schasfoort, Trends in miniaturized total analysis systems for point-of-care testing in clinical chemistry, *Lab Chip*, 2001, **1**, 2, 83–95.
11 H. A. Stone, A. D. Stroock and A. Ajdari, Engineering flows in small devices: Microfluidics towards a lab-on-a-chip, *Ann. Rev. Fluid Mech.*, 2004, **36**, 381–411.
12 D. Figeys and D. Pinto, Lab-on-a-chip: A revolution in biological and medical sciences, *Anal. Chem.*, 2000, **72**, 9, 330–335A.
13 M. Madou and G. Kellogg, LabCD: A Centrifuge-Based Platform for Diagnostics, *Proceedings of the International SPIE Conference*, San Jose, 1998, The International Society of Optical Engineering, Bellingham, USA, 1998, vol. 3259, pp. 80–93.
14 C. Schembri, T. Burd, A. Kopf-Sill, L. Shea and B. Braynin, Centrifugation and capillarity integrated into a multiple analyte whole-blood analyzer, *J. Autom. Chem.*, 1995, **17**, 3, 99–104.
15 M. Madou, Y. Lu, S. Lai, J. Lee and S. A. Daunert, A centrifugal microfluidic platform: A comparison, micro total analysis systems, *Proceedings of the 4th International μTAS Conference*, Enschede, 2000, Kluwer Academic Publishers, Dodrecht, The Netherlands, 2000, pp. 565–570.
16 D. C. Duffy, H. L. Gills, J. Lin, N. F. Sheppard and G. J. Kellogg, Microfabricated centrifugal microfluidic systems: characterization and multiple enzymatic assays, *Anal. Chem.*, 1999, **71**, 20, 4669–4678.
17 M. Madou, L. Lee, S. Daunert, S. Lai and C. Shih, Design and fabrication of CD-like microfluidic platforms for diagnostics: Microfluidic Functions, *Biomed. Microdevices*, 2001, **3**, 3, 245–254.
18 M. Madou, Y. Lu, S. Lai, C. Koh, L. J. Lee and B. R. Wenner, A novel design on a CD for 2-point measurement, *Sens. Actuators, A*, 2001, **91**, 301–306.
19 S. Lai, S. Wang, J. Luo, L. Lee, S. Yang and M. Madou, Design of a compact disk-like microfluidic platform for enzyme-linked immunosorbent Assay, *Anal. Chem.*, 2004, **76**, 1832–1837.
20 G. Ekstrand, C. Holmquist, A. E. Oerleforn, B. Hellmann, A. Larsson and P. Andersson, Microfluidics in a rotating CD, *Proceedings of the 4th International μTAS Conference*, Enschede, 2000, Kluwer Academic Publishers, Dodrecht, The Netherlands, 2000, pp. 311–314.
21 G. Thorsén, G. Ekstrand, U. Selditz, S. R. Wallenborg and P. Andersson, Integrated Microfluidics for parallel processing of proteins in a CD microlaboratory, *Proceedings of the 7th International μTAS Conference*, Squaw Valley, 2003, MESA Monographs, Squaw Valley, USA, 2003, pp. 457–460.
22 J. Ducrée, T. Brenner, M. Grumann, W. Bessler, M. Stelzle, S. Messner, T. Nann, J. Rühe, I. Moser and R. Zengerle, *Bio-Disk – A Centrifugal Platform for Integrated Point-of-Care Diagnostics on Whole Blood*, 2003, http://www.bio-disk.com.
23 J. Steigert, M. Grumann, T. Brenner, K. Mittenbühler, T. Nann, J. Rühe, I. Moser, S. Haeberle, L. Riegger, J. Riegler, W. Bessler, R. Zengerle and J. Ducrée, Integrated Sample Praparation, Reaction and Detection on a High-Frequency Centrifugal Microfluidic Platform, *JALA*, 2005, **10**, 5, 331–341.
24 Piccolo, Abaxis Inc., 3240 Whipple Road, 94587 Union City, CA, USA, http://www.abaxis.com, accessed May 2005.
25 Gyrolab Bioaffy CD, Gyros AB, Dag Hammarskjölds väg 54, SE-751 83 Uppsala, Sweden (formerly Pharmacia Inc., USA), http://www.gyros.com, accessed June 2005.
26 M. Inganäs, H. Derand, A. Eckersten, G. Ekstrand, A. K. Honerud, G. Jesson, G. Thorsén, T. Söderman and P. Andersson, *An integrated microfluidic CD device with potential utility in both centralized and POC laboratory settings*, Gyros AB, Dag Hammarskjölds väg 54, SE-751 83 Uppsala, Sweden, http://www.gyros.de, accessed June 2005.
27 GyrolabTM Maldi SP1, Gyros AB, Dag Hammarskjölds väg 54, SE-751 83 Uppsala, Sweden, http://www.gyros.de, accessed June 2005.
28 Bio-CD, Eppendorf AG, Barkhausendweg 1, 22339 Hamburg, Germany, http://www.eppendorf.de, accessed June 2005.
29 SpinX Technologies, Rue Lect 29, 1217 Geneva, Switzerland, http://www.spinx-technologies.com, accessed June 2005.
30 C. T. Schembri, *U.S. Pat.*, 5 473 603, 1993.
31 E. Verpoorte, Chip vision – Optics for microchips, *Lab Chip*, 2003, **3**, 42N–52N.
32 E. Verpoorte, A. Manz, H. Lüdi, A. E. Bruno, F. Maystre, B. Krattinger, H. M. Widmer, B. H. van der Schoot and N. F. de Rooij, A silicon flow cell for optical detection in miniaturized total chemical analysis systems, *Sens. Actuators, B*, 1992, **6**, 66–70.
33 B. Splawn and F. Lytle, On-chip absorption measurement using integrated wave guides, *Anal. Bioanal. Chem.*, 2002, **373**, 519–525.
34 J. Roulet, R. Völkel, H. Herzig, E. Verpoorte and N. de Rooij, Fabrication of multilayer systems combining microfluidic and microoptical elements for fluorescence detection, *J. Microelectromech. Syst.*, 2001, **10**, 482–491.
35 Z. Liang, N. Chiem, G. Ocvirk, T. Tang, K. Fluri and D. J. Harrison, Microfabrication of a planar absorbance and fluorescence cell of integrated capillary electrophoresis devices, *Anal. Chem.*, 1996, **68**, 1040–1046.
36 N. Petersen, K. Mogensen and J. Kutter, Performance of an in-plane detection cell with integrated waveguides for UV/VIS absorbance measurement on microfluidic separation devices, *Electrophoresis*, 2002, **23**, 3528–3536.
37 A. Manz and E. Verpoorte, *U.S. Pat.*, 5 599 503, 1997.
38 E. S. Yeung and R. E. Synovec, Detectors for liquid chromatography, *Anal. Chem.*, 1986, **58**, 12, 1237A–1256A.
39 X. Xi and E. S. Yeung, Axial-beam on-column absorption detection for open tubular capillary liquid chromatography, *Anal. Chem.*, 1990, **62**, 1580–1585.
40 M. Grumann, I. Moser, J. Steigert, L. Riegger, A. Geipel, C. Kohn, G. Urban, R. Zengerle and J. Ducrée, Optical beam guidance in monolithic polymer chips for miniaturized colorimetric assays, *Proceedings of the 18th IEEE Conference on MEMS*, Miami, 2005, Institute of Electrical and Electronics Engineers, Inc., Piscataway, USA, 2005, pp. 108–112.
41 Flexpoint 532 nm, Laser Components IG, Inc., USA, http://www.laser-components.com, accessed September 2004.
42 UV/VIS Microspectrometer, Boehringer Ingelheim MicroParts AG, Germany, http://www.microparts.de, accessed October 2004.
43 ALK 121, Diaglobal GmbH, Germany, http://www.diaglobal.de, accessed January 2005.
44 J. Zeng, D. Banerjee, M. Deshpande, J. Gilbert, C. D. Duffy and D. J. Kellogg, Design analysis of capillary burst valves in centrifugal microfluidics, *Proceedings of the 4th International μTAS Conference*, Enschede, 2000, Kluwer Academic Publishers, Dodrecht, The Netherlands, 2000, pp. 579–582.
45 M. R. Mc Neely, M. K. Spute, N. A. Tusneem and A. R. Oliphjat, Hydrophobic microfluidics, *Proceedings of the International SPIE Conference*, Santa Clara, 1999, The International Society of Optical Engineering, Bellingham, USA, 1999, vol. 3877, pp. 210–220.
46 M. Grumann, T. Brenner, C. Beer, R. Zengerle and J. Ducrée, Visualization of flow patterning in high-speed centrifugal microfluidics, *Rev. Sci. Instrum.*, 2005, **76**, 2, 025101-1–025101-6.
47 T. Brenner, PhD thesis, *Polymer Fabrication and Microfluidic Unit Operations for Medical Diagnostics on a Rotating Disk*, University of Freiburg–IMTEK, 2005.
48 *EP Pat.*, 0 596 104 B1, 1993.
49 *EP Pat.*, 1 019 193 B1, 1998.
50 *DE Pat.*, 10 2004 009 012 A1, 2004.
51 M. Grumann, A. Geipel, L. Riegger, R. Zengerle and J. Ducrée, Batch-mode mixing with magnetic beads on centrifugal microfluidic platforms, *Lab Chip*, 2005, **5**, 560–565.
52 ALK QS, Diaglobal GmbH, Germany, http://www.diaglobal.de, accessed January 2005.
53 Vario-Photometer, Diaglobal GmbH, Germany, http://www.diaglobal.de, accessed January 2005.
54 HSG-IMIT, Institut für Mikro- und Informationstechnik der Hahn-Schickard-Gesellschaft e.V., Wilhelm-Schickard Strasse 10, D-78052 Villingen Schwenningen, Germany, http://www.hsg-imit.de, accessed April 2005.
55 Jobst-Technologies GmbH, Georges-Koehler Allee 102, D-79110 Freiburg, Germany, http://www.jobst-technologies.com, accessed April 2005.

